Noise propagation in a class of metabolic networks

A. Borri P. Palumbo A. Singh

Abstract— **A metabolic pathway made of a cascade of biochemical reactions is considered, with a substrate which is eventually transformed into the final product by means of a sequence of reactions, each catalyzed by the same enzyme. The amount of the enzyme varies according to discrete noisy processes of production and elimination. A feedback acts on the final product clearance rate, exerted by the final product accumulation itself: higher final product levels lead to a faster dynamics. The aim of this note is to investigate how the noise scales with the length of the cascade and how the feedback impacts on the noise propagation. To this end, a Stochastic Hybrid System (SHS) formulation is exploited, with the enzyme production/clearance processes constituting the noise source. The noise propagation is measured in terms of the square of the coefficient of variation of the final product, and computations are carried out by means of the equations of moments, which are estimated in closed form after linearizing the SHS. Analytical solutions allow to infer information and to relate the noise propagation to the model parameters. Similarly to recent results occurring in other types of enzymatic reactions, the results highlight the influential role of feedback in noise reduction.**

Index Terms— **Metabolic pathways, Moment Equations, Negative Feedback**

I. Introduction

In the last few years, mathematical control theory has been increasingly applied in Systems and Synthetic Biology. On the one hand, the aim of Systems Biology is to understand, quantify and conceptualize the diverse frameworks involving complex biological systems, possibly taking inspiration from established engineering paradigms: one may cite, among the others, the role of feedback, which has been widely investigated, especially in transcriptional and metabolic regulation where gene products are required to control their homeostatic levels robustly with respect to parameter or environmental fluctuations [1], [2], [3], [4], [5], [6], [7], [8], [9], [10], [11]; on the other hand, Synthetic Biology aims at merging molecular biological techniques with mathematical modeling and forward engineering in order to design synthetic biological circuits, able to replicate emergent properties potentially useful for biotechnology industry, human health and environment (see [12], [13], [14], [15], [16] and references therein).

This note considers the case of a metabolic pathway, with a substrate p_0 undergoing a cascade of n metabolic modifications, leading to the final product p_n. Substrate production and final product clearance are also accounted for, see the scheme in Fig. 1. Each substrate modification is catalyzed by enzymes: the assumption is that there exists only one enzyme acting on all the biochemical reactions. The amount of the enzyme varies according to discrete noisy processes of production and elimination. One may think at the proposed scheme as to a simplified paradigm for a wide range of sequential events like, e.g. cascades of phosphorylations. The final product accumulation acts in feedback to speed up its own dynamics. This fact has been recently investigated in [17] at a single-cell level, where an apparent correlation between the metabolic level and the growth rate has been highlighted, while a similar cascade scheme, related to gene expression, was investigated in a different fashion in [18].

The aim of this note is to investigate how the noise scales with the length n of the cascade and how the feedback impacts on the noise propagation. To this end a Stochastic Hybrid System (SHS) is exploited, with the enzyme updates (production and clearance) being the only noise sources of the system. Noise is measured in terms of the squared coefficient of variation of the final product. Computations are carried out by means of the moment equations [19], [20], [21]: because of the nonlinearities involved by the Ordinary Differential Equation (ODE) system associated to the SHS, computations are made after linearization, so that the moment equations come out in closed form. Despite the simplifications adopted, an explicit easy-to-handle solution is not provided, in favor of a recursive algorithm releasing the second-order moment associated to p_n. Results coming after linearization are validated by the Gillespie Stochastic Simulation Algorithm (SSA), run according to the original nonlinear system, which is shown to be very close to the approximated one on a wide range of model parameters.

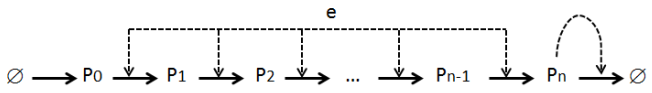

Fig. 1. Cascade of biochemical reactions.

Similarly to recent results occurring in other types of enzymatic reactions [7], [9], [10], [8], results highlight the influential role of the feedback in noise reduction.

The note is organized as follows. Section 2 is devoted to introduce the SHS mathematical model describing the metabolic pathway. First and second order moments are computed in Sections 3 and 4, showing how they are related to the model and feedback parameters. Section 3 is devoted

A. Borri, and P. Palumbo are with the Istituto di Analisi dei Sistemi e Informatica "A. Ruberti", Italian National Research Council (IASI-CNR), Via dei Taurini, Roma, Italy. Email addresses: {alessandro.borri, pasquale.palumbo}@iasi.cnr.it

A. Singh is with Department of Electrical and Computer Engineering, Biomedical Engineering, Mathematical Sciences, Center for Bioinformatics and Computational Biology, University of Delaware, Newark, DE USA 19716. E-Mail address: absingh@udel.edu

TABLE I
CHEMICAL REACTIONS.

Event	Enzyme reset	Propensity function
Enzyme production	$e(t) \mapsto e(t)+1$	$a_1 = k_e$
Enzyme clearance	$e(t) \mapsto e(t)-1$	$a_2 = \gamma_e e(t)$

to introducing the linear approximation as well, which is achieved in the neighborhood of the steady-state of the system. Section 5 reports simulation results carried out in order to stress the improvements in noise reduction achieved by the feedback.

II. METABOLIC PATHWAY MODEL

Consider the scheme in Fig. 1, where a substrate is sequentially modified n times passing from *state 0*, to *state 1* and, eventually, to *state* n. These modifications are supposed irreversible. Denote with p_i, $i = 0, 1, \ldots, n$ the copy number of the substrate in *state* i. By assuming standard mass-action law to describe the substrate modifications catalyzed by a unique enzyme (whose copy number is denoted by e), the ODE system associated to the metabolic pathway under investigation is:

$$\begin{aligned} \tfrac{dp_0}{dt} &= k_p - \tfrac{\lambda}{e^\star} e(t) p_0(t) \\ \tfrac{dp_i}{dt} &= \tfrac{\lambda}{e^\star} e(t) p_{i-1}(t) - \tfrac{\lambda}{e^\star} e(t) p_i(t) \qquad i = 1, \ldots, n-1 \\ \tfrac{dp_n}{dt} &= \tfrac{\lambda}{e^\star} e(t) p_{n-1}(t) - \gamma_p p_n(t) \end{aligned} \tag{1}$$

where k_p stands for the p_0 substrate production rate, λ is the rate of transformation from p_i into p_{i+1} (and is normalized by the average steady-state enzyme copy number, denoted by $e^\star$) and γ_p stands for the final product clearance rate.

Motivated by [17], where an apparent correlation between the metabolic level and the growth rate has been highlighted, we introduce a feedback action exerted by the final product accumulation on the clearance rate γ_p, according to the following Hill function:

$$\gamma_p(p_n) = \bar{\gamma}_p \frac{p_n^h}{\theta^h + p_n^h}, \tag{2}$$

where $\bar{\gamma}_p$ is the *clearance strength*, providing the maximal clearance rate, obtainable for negligible values of the repression threshold θ (negligible w.r.t. the p_n copy number), θ indicates half of the maximal value reached for $p_n = \theta$, and parameter h is the *feedback sensitivity*, providing the steepness of the sigmoidal function.

The copy number of the enzyme acting at catalyzing the substrate transformation is allowed to vary according to discrete noisy processes of production and clearance, whose related chemical reactions are summarized in Table I, detailing the resets on the enzyme and the propensities associated to both production/clearance processes.

In the following, unless differently specified, the expected value of a random variable x is denoted by $\langle x \rangle$, while the steady-state of the average of a stochastic process $x(t)$ and of a second-order moment $\langle x(t)y(t) \rangle$ are denoted by $x^\star = \lim_{t \mapsto +\infty} \langle x(t) \rangle$ and $\langle xy \rangle^\star = \lim_{t \mapsto +\infty} \langle x(t)y(t) \rangle$, respectively.

A. Metabolic noise computation

In order to quantify how the noise scales with respect to the length of the metabolic pathway and the feedback action, we define the *metabolic noise* associated to the final product p_n by means of the square of the coefficient of variation $CV^2_{p,n}$, computed by the ratio:

$$CV^2_{p,n} = \sigma^2_n / (p^\star_n)^2, \tag{3}$$

where σ^2_n and $p^\star_n$ are the steady-state values for variance and mean of the marginal distribution of the final product p_n copy number. It readily comes out that, by varying the model or the feedback parameters, $CV^2_{p,n}$ may vary because of both the p_n steady-state and the fluctuations around $p^\star_n$. Moreover, in order to compare the *feedback* and the *no-feedback* cases, the *feedback relative noise* is defined as the ratio

$$\eta^2_n = \frac{CV^2_{p,n}(feedback)}{CV^2_{p,n}(no\ feedback)} \tag{4}$$

where the *no-feedback* case refers to $\gamma_p(p_n) = \bar{\gamma}_p$, a situation occurring whenever the final product copy number is much larger than the threshold: $p_n \gg \theta$.

III. AVERAGE STEADY-STATE SOLUTIONS

The first-order moment equations associated to the SHS modeling the reaction schemes are derived from [19]. Since the enzyme is not influenced by the substrate, any order moment of e can be computed without any approximation, readily providing the following results for the equilibrium first- and second-order moments:

$$e^\star = \frac{k_e}{\gamma_e}, \qquad \left\langle e^2 \right\rangle^\star = (e^\star)^2 + e^\star, \tag{5}$$

from which it comes that

$$CV^2_e = \frac{\left\langle e^2 \right\rangle^\star - (e^\star)^2}{(e^\star)^2} = \frac{1}{e^\star} = \frac{\gamma_e}{k_e}. \tag{6}$$

As expected, the noise source becomes larger by reducing the average enzyme copy number.

On the other hand, the first-order moment equations applied to the SHS provide the following identities

$$\begin{aligned} &\langle ep_0 \rangle^\star = \langle ep_1 \rangle^\star = \cdots = \langle ep_{n-1} \rangle^\star = \tfrac{k_p e^\star}{\lambda} \\ &\langle \gamma_p(p_n) p_n \rangle^\star = \tfrac{\lambda}{e^\star} \langle ep_{n-1} \rangle^\star = k_p \end{aligned} \tag{7}$$

which do not allow any closed-form solutions because of the nonlinearities involved in the ODE associated to the SHS. To cope with this drawback, we linearize (around the steady states $e^\star$ and $p^\star_n$) the nonlinear function $\gamma_p(p_n)p_n$ as well as the mass-action law related to the intermediate substrate transformations, so that the ODE system associated to the

SHS becomes:

$$\begin{aligned}
\tfrac{dp_0}{dt} &= k_p - \tfrac{\lambda p_0^\star}{e^\star} e(t) - \lambda(p_0(t) - p_0^\star) \\
\tfrac{dp_i}{dt} &= \tfrac{\lambda p_{i-1}^\star}{e^\star} e(t) + \lambda(p_{i-1}(t) - p_{i-1}^\star) \\
&\quad - \tfrac{\lambda p_i^\star}{e^\star} e(t) - \lambda(p_i(t) - p_i^\star) \qquad i = 1, \ldots, n-1 \\
\tfrac{dp_n}{dt} &= \tfrac{\lambda p_{n-1}^\star}{e^\star} e(t) + \lambda(p_{n-1}(t) - p_{n-1}^\star) - \gamma_p(p_n^\star) p_n^\star \\
&\quad - \big(\gamma_p(p_n^\star) + p_n^\star \gamma_p'(p_n^\star)\big)(p_n(t) - p_n^\star).
\end{aligned} \tag{8}$$

Then, first-order moment equations readily provide the following solutions:

$$p_0^\star = p_1^\star = \cdots = p_{n-1}^\star = \frac{k_p}{\lambda}, \tag{9}$$

with the steady-state solution $p_n^\star$ satisfying the following nonlinear equation

$$\varphi(p_n^\star) = \gamma_p(p_n^\star) p_n^\star - k_p = 0. \tag{10}$$

In fact, (10) admits a unique positive solution, since $\varphi(p_n^\star = 0) = -k_p < 0$, $\lim_{p_n^\star \mapsto +\infty} \varphi(p_n^\star) = +\infty$ and $\varphi'(p_n^\star) > 0$ for any positive $p_n^\star$: by continuity there exists a unique positive real $p_n^\star$ that satisfies (10).

Remark 1: According to (9)–(10), it comes out that the first-order steady-state solutions $p_0^\star, p_1^\star, \ldots, p_n^\star$ do not depend of the length n of the cascade. To avoid confusion, in the following, $p_n^\star$ will be shortly denoted by ϱ, without the possibly misleading suffix n.

Because of (9)–(10), the linearized system (8) simplifies into:

$$\begin{aligned}
\tfrac{dp_0}{dt} &= k_p - \tfrac{\lambda p_0^\star}{e^\star} e(t) - e^\star(p_0(t) - p_0^\star) \\
\tfrac{dp_i}{dt} &= \lambda\big(p_{i-1}(t) - p_i(t)\big), \qquad i = 1, \ldots, n-1 \\
\tfrac{dp_n}{dt} &= \tfrac{\lambda p_{n-1}^\star}{e^\star} e(t) + \lambda(p_{n-1}(t) - p_{n-1}^\star) - k_p \\
&\quad - \big(\gamma_p(p_n^\star) + p_n^\star \gamma_p'(p_n^\star)\big)(p_n(t) - p_n^\star).
\end{aligned} \tag{11}$$

It's worth noticing that intermediate average steady-states do not vary with the feedback, nor with the length of the cascade. Instead, by varying the clearance strength $\bar{\gamma}_p$ and the feedback parameters θ and h, the average steady-state solution ϱ varies as described next (it can be readily verified by accounting for the fact the solution to (10) is the (unique) intersection of a fixed hyperbola, k_p/ϱ, with the Hill function, $\gamma_p(\varrho)$, associated to the feedback).

i) Keeping fixed the other parameters, if one increases the clearance strength $\bar{\gamma}_p$, then ϱ reduces; instead, for $\bar{\gamma}_p \mapsto 0^+$, the solution ϱ becomes larger and larger, and it tends to coincide with the solution without feedback for $\varrho \gg \theta$. Fig. 2 shows on a log-scale how ϱ varies according to 4 different feedback sensitivities.

$$\lim_{\bar{\gamma}_p \mapsto +\infty} p_n^\star = 0, \qquad \lim_{\bar{\gamma}_p \mapsto 0^+} p_n^\star = +\infty. \tag{12}$$

ii) Keeping fixed the other parameters, if one increases the threshold θ, then ϱ increases; instead, for $\theta \mapsto 0^+$, the solution ϱ tends to coincide with the one without feedback since $\varrho \gg \theta$. Fig. 3 shows on a log-scale how ϱ varies according to 4 different feedback sensitivities.

$$\lim_{\theta \mapsto +\infty} p_n^\star = +\infty, \qquad \lim_{\theta \mapsto 0^+} p_n^\star = \frac{k_p}{\bar{\gamma}_p}. \tag{13}$$

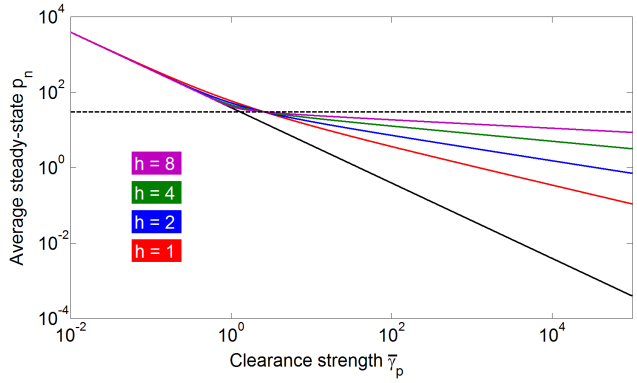

Fig. 2. Average steady-state of p_n by varying the clearance strength $\bar{\gamma}_p$. The black line provides the solution without feedback that lower bounds the other feedback solutions and gets closer and closer to the feedback solutions according to a threshold $\theta \ll \varrho$. Fixed parameters (k_p, k_e, γ_e, θ, λ) are reported in Table II.

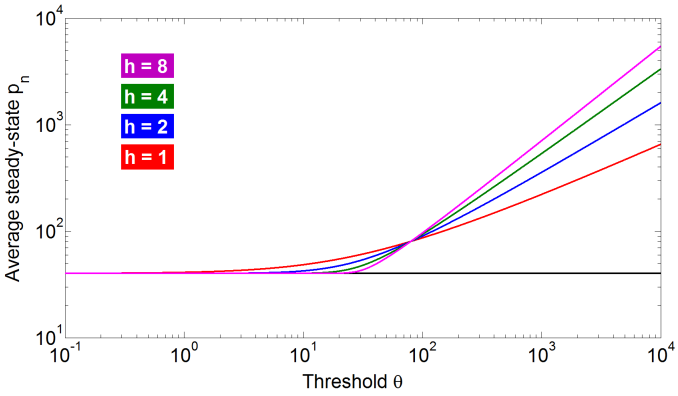

Fig. 3. Average steady-state of p_n by varying the feedback threshold θ. The black line provides the solution without feedback, which lower bounds the other feedback solutions and gets closer and closer to the feedback solutions according to a threshold $\theta \ll \varrho$. Fixed parameters (k_p, k_e, γ_p, γ_e, λ) are reported in Table II.

In summary, with respect to the average steady-state solutions, the effect of feedback is exerted only on the final product $p_n^\star$, providing an increase (with respect to the no-feedback case) which is sharpened by increasing the feedback sensitivity h. The length of the cascade does not affect the average steady-state.

IV. Second Order Moments

The computation of the metabolic noise defined in (3) and (4) requires $\langle p_n^2 \rangle^\star$. To this end, we need an algorithm to obtain the second order moments associated to (11). According to the linear fashion of (11), these moments will

TABLE II

MODEL PARAMETERS. MEASUREMENTS UNITS: k_p, k_e [MOLECULES/TIME], λ, γ_e, $\bar{\gamma}_p$ [TIME^{-1}], θ [MOLECULES]

Parameter	k_p	k_e	λ	$\bar{\gamma}_p$	γ_e	θ
Value	40	10	10	1	1	30

be found in closed form. To this end, denote

$$\frac{dp_i}{dt} = f_i\big(p_{i-1}, p_i, e\big), \qquad i = 0, 1, \dots, n, \tag{14}$$

the generic linear equation associated to the state p_i in (11). Then, the following identities are derived from [19] when setting equal to zero the second order dynamics for $i, j, = 0, 1, \dots, n$:

$$\frac{d\left\langle ep_i\right\rangle}{dt} = 0 \quad \Longrightarrow \quad \left\langle e f_i\big(p_{i-1}, p_i, e\big)\right\rangle + k_e p_i - \gamma_e \left\langle ep_i\right\rangle = 0 \tag{15}$$

$$\frac{d\langle p_i p_j\rangle}{dt} = 0 \quad \Longrightarrow \quad \left\langle p_j f_i\big(p_{i-1}, p_i, e\big)\right\rangle + \left\langle p_i f_j\big(p_{j-1}, p_j, e\big)\right\rangle = 0 \tag{16}$$

providing a square linear system of $n + 1 + \frac{(n+1)(n+2)}{2}$ algebraic equations with respect to the unknowns $\left\langle ep_i\right\rangle^\star$, $\langle p_i p_j\rangle^\star$. Below are provided the steps to compute $\left\langle p_n^2\right\rangle^\star$.

Step 1. From (15), the second-order moments $\left\langle ep_i\right\rangle^\star$ are found to satisfy the following closed form equation:

$$\left\langle ep_i\right\rangle^\star = e^\star p_i^\star \left(1 - \alpha^{i+1} \cdot CV_e^2\right) \tag{17}$$

for $i = 0, 1, \dots, n-1$, with

$$\alpha = \frac{\lambda}{\lambda + \gamma_e}, \tag{18}$$

whilst $\left\langle ep_n\right\rangle^\star$ is provided by

$$\left\langle ep_n\right\rangle^\star = e^\star \varrho^\star \left(1 + \frac{\gamma_p(\varrho)(1-\alpha^n)}{\gamma_e + \Gamma(\varrho)} \cdot CV_e^2\right), \tag{19}$$

where

$$\Gamma(\varrho) = \gamma_p(\varrho) + \varrho \gamma_p'(\varrho). \tag{20}$$

Remark 2: According to its definition in (18), it results $\alpha < 1$. As a matter of fact, long pathways share the same insensitivity of $\left\langle ep_n\right\rangle^\star$ to n, since for n large enough, one has $\alpha^n \simeq 0$ and (19) simplifies into

$$\left\langle ep_n\right\rangle^\star \simeq e^\star \varrho^\star \left(1 + \frac{\gamma_p(\varrho)}{\gamma_e + \Gamma(\varrho)} \cdot CV_e^2\right). \tag{21}$$

The length of the cascade such that (21) is a good approximation of (19) depends on the enzyme dynamics. If we increase the propensities of e without varying its average steady-state $e^\star$ (i.e. if we proportionally increase both k_e and γ_e), then λ does not vary either (because it refers to the rate of modification normalized by a fixed value $e^\star$) and α becomes smaller. The result is that, by increasing the frequency at which the enzyme copy number varies (keeping fixed $e^\star$), then the *long-cascade* approximation (21) becomes accurate for smaller n.

Step 2. By properly exploiting the equations for $\langle p_0 p_i\rangle$, $i = 0, 1, \dots, n$ in (16), we find the following recursive linear system

$$\langle p_0 p_{i+1}\rangle^\star = \tfrac{1}{2}\langle p_0 p_i\rangle^\star + \tfrac{p_0^\star p_i^\star}{2}\left(1 + \alpha^{i+2} \cdot CV_e^2\right), \quad i = 0, 1, \dots, n-2, \tag{22}$$

$$\langle p_0 p_n\rangle^\star = \tfrac{\lambda}{\lambda + \Gamma(\rho)}\langle p_0 p_{n-1}\rangle^\star + p_0^\star \varrho \left(1 - \tfrac{\gamma_p(\varrho)}{\lambda + \Gamma(\varrho)}\right) - \tfrac{p_0^\star \varrho \gamma_p(\varrho)}{\lambda + \Gamma(\varrho)}\left(\tfrac{\lambda(1-\alpha^n)}{\gamma_e + \Gamma(\varrho)} - \alpha\right) CV_e^2, \tag{23}$$

with initial condition

$$\left\langle p_0^2\right\rangle^\star = (p_0^\star)^2\left(1 + \alpha \cdot CV_e^2\right). \tag{24}$$

The $n-1$ equations in (22) are recursively solved providing

$$\langle p_0 p_{n-1}\rangle^\star = p_0^\star p_{n-1}^\star + \frac{\alpha p_0^\star p_{n-1}^\star}{2^{n-1}}\left(1 + \alpha \frac{1 - (2\alpha)^{n-1}}{1 - 2\alpha}\right) CV_e^2. \tag{25}$$

By substituting (25) into (23), we obtain $\langle p_0 p_n\rangle^\star$:

$$\langle p_0 p_n\rangle^\star = p_0^\star \varrho + \tfrac{p_0^\star \varrho \gamma_p(\varrho)}{\lambda + \Gamma(\varrho)}\left(\tfrac{\alpha}{2^{n-1}}\left(1 + \alpha \tfrac{1-(2\alpha)^{n-1}}{1-2\alpha}\right) - \tfrac{\lambda(1-\alpha^n)}{\gamma_e + \Gamma(\varrho)} + \alpha\right) CV_e^2. \tag{26}$$

Similarly to what has been said in Remark 2, for n large enough we have that $\langle p_0 p_n\rangle^\star$ can be approximated by the limit

$$\langle p_0 p_n\rangle^\star \simeq p_0^\star \varrho \left(1 - \frac{\lambda \gamma_p(\varrho)(\lambda - \Gamma(\varrho))}{(\lambda + \Gamma(\varrho))(\gamma_e + \Gamma(\varrho))(\lambda + \gamma_e)} CV_e^2\right). \tag{27}$$

Step 3. We compute the steady-state solutions for $\langle p_i p_j\rangle$, with $i = 1, \dots, n$, $j = 1, \dots, n-1$, according to the following Lemma.

Lemma 3: Let $k = 0, 1, \dots, n-1$ and define

$$X_k = \begin{bmatrix} \langle p_1 p_k\rangle^\star \\ \vdots \\ \langle p_n p_k\rangle^\star \end{bmatrix} \in \mathbb{R}^n. \tag{28}$$

Then, X_k obeys the following recursive linear equation for $k = 0, 1, \dots, n-2$:

$$X_{k+1} = A(\varrho) X_k + B(\varrho) U_k, \tag{29}$$

where

$$\begin{aligned} A(\varrho) &= \big(I_n - A_2(\varrho)\big)^{-1} A_1(\varrho), \\ B(\varrho) &= \big(I_n - A_2(\varrho)\big)^{-1} B_1, \end{aligned} \tag{30}$$

with I_n the identity matrix in $\mathbb{R}^{n\times n}$ and

$$A_1(\varrho) = \operatorname{diag}\left\{\frac{1}{2}, \frac{1}{2}, \cdots, \frac{1}{2}, \frac{\lambda}{\lambda + \Gamma(\varrho)}\right\}, \tag{31}$$

$A_2(\varrho) \in \mathbb{R}^{n\times n}$, $B_1 \in \mathbb{R}^{n\times 2}$ matrices with the only nontrivial elements given by

$$\begin{aligned} &A_2(i, i-1) = \tfrac{1}{2}, \qquad i = 2, 3, \dots, n-1, \\ &A_2(n, n-1) = \tfrac{\lambda}{\lambda + \Gamma(\varrho)}, \quad B_1(1,1) = \tfrac{1}{2}, \quad B_1(n,2) = 1. \end{aligned} \tag{32}$$

The input U_k in (29) is defined by

$$U_k = \begin{bmatrix} \langle p_0 p_{k+1} \rangle^\star \\ \frac{p_0 \varrho}{\lambda + \Gamma(\varrho)} \left(\varrho \gamma_p'(\varrho) - \gamma_p(\varrho) \alpha^{k+1} \cdot CV_e^2 \right) \end{bmatrix}. \quad (33)$$

Proof: The proof comes straightforwardly by computing the second order moments from (16), according to which:

$$X_{k+1} = A_1(\varrho) X_k + A_2(\varrho) X_{k+1} + B_1(\varrho) U_k. \quad (34)$$

■

Lemma 3, together with the initial conditions X_0 provided by Step 2, allows to formally write the explicit solution for X_{n-1}:

$$X_{n-1} = A(\varrho)^{n-1} X_0 + \sum_{k=0}^{n-2} A(\varrho)^{n-k-2} B(\varrho) U_k, \quad (35)$$

from which the second order moment $\langle p_n p_{n-1} \rangle^\star$ is given by the last component of X_{n-1}.

According to Remark 2, for n large enough, X_{n-1} does not depend any more of X_0 (the first term in (35) can be neglected), since matrix $A(\varrho)$ has all positive eigenvalues and in the unit circle (indeed, the spectrum of A coincides with the spectrum of A_1, as it can be readily seen by the triangular shape of the matrices). Unfortunately, no apparent easy-to-handle solutions are available for $\langle p_n p_{n-1} \rangle^\star$, even according to simplifying assumption of large n.

Step 4. The last step consists in the computation of $\langle p_n^2 \rangle^\star$, coming from (16) written for $i = j = n$. Then, after computations:

$$\langle p_n^2 \rangle^\star = \varrho^2 \cdot \left(1 - \frac{\gamma_p(\varrho)}{\Gamma(\varrho)} \right) + \frac{\lambda}{\Gamma(\varrho)} \langle p_n p_{n-1} \rangle^\star + \frac{k_p^2 (1 - \alpha^n)}{\Gamma(\varrho) \left(\gamma_e + \Gamma(\varrho) \right)} \cdot CV_e^2, \quad (36)$$

with $\langle p_n p_{n-1} \rangle^\star$ achieved in Step 3. $CV_{p,n}^2$ is straightforwardly computed according to (3).

Remark 4: In summary, with respect to the way the noise scales with the length of the metabolic pathway, analytical solutions for the second-order moments highlight the fact that the influence of n is related to the value of the proper fraction α, since n appears in the moments computations in the form of α^n. The values of $CV_{p,n}^2$ converge to a limit point when $n \mapsto +\infty$, according to a rate given by α: the smaller is α (i.e. the closer to zero), the faster is the rate. As previously stated in Remark 2, α is related to the enzyme dynamics.

The way the feedback influences the noise propagation will be discussed by simulations in the next section.

V. Numerical Simulations

Numerical simulations have been carried out in order to evaluate how the feedback scales with noise propagation. Figs. 4 and 5 report the standard deviation according to different values of the clearance strength $\bar{\gamma}_p$ and of the threshold θ. Other parameters can be found in Table II. Continuous lines refer to the shortest cascade with only p_0, p_1, p_2, whilst dotted lines refer to the case of $n = 12$. Parameters are set providing $\alpha = 10/11$ closer to 1 than to 0, thus allowing the length n to play a nontrivial role. By comparing Figs. 4–5 with Figs. 2–3 it is apparent that for values of $\bar{\gamma}_p$ (and of θ) small enough to provide an average steady-state $\varrho \gg \theta$, the feedback does not exert a real action (because the Hill function in (2) can be confused with $\bar{\gamma}_p$) and the standard deviation without the feedback (black line) is not modified by the feedback (colored lines). Instead, by increasing $\bar{\gamma}_p$ in Fig. 4 (and θ in Fig. 5), the feedback exerts its action and both figures show an overall increase in σ, with the curves showing non-monotonicity for the feedback sensitivity $h > 1$. However, this fact does not provide a corresponding increase in the metabolic noise (quantified by the coefficient of variation defined in (3)) because the feedback leads also to an increment of the steady-state ϱ. This fact can be appreciated by the plot of the *feedback relative noise* (4), where it is apparent (in Figs. 6–7) how the feedback strongly reduces η_n^2 according to a monotonic decrease, which becomes sharper by increasing the feedback sensitivity h.

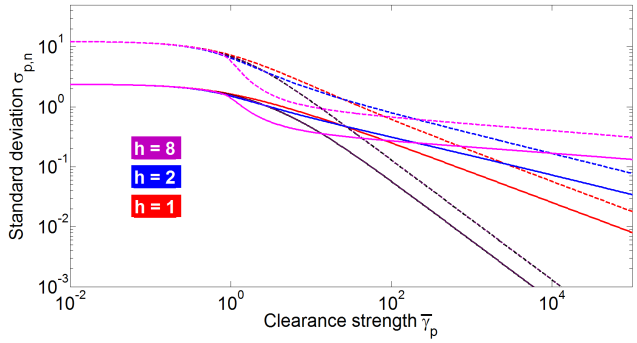

Fig. 4. Standard deviation of p_n by varying the clearance strength $\bar{\gamma}_p$. The black line provides the solution without feedback. Fixed parameters (k_p, k_e, γ_e, θ, λ) are reported in Table II. Continuous lines refer to $n = 2$; dotted lines refer to $n = 12$.

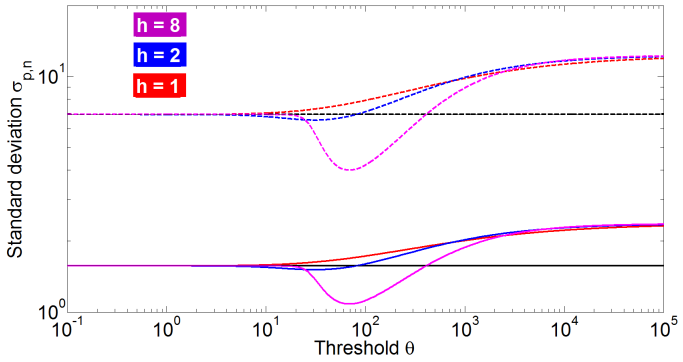

Fig. 5. Standard deviation of p_n by varying the feedback threshold θ. The black line provides the solution without feedback. Fixed parameters (k_p, k_e, γ_p, γ_e, λ) are reported in Table II. Continuous lines refer to $n = 2$; dotted lines refer to $n = 12$.

Finally, Figs. 8–9 report numerical results on the steady-state ϱ and $\langle p_n^2 \rangle^\star$ computed by means of the Gillespie Stochastic Simulation Algorithm (SSA) [22], properly modified to take into account the SHS framework. Stochastic

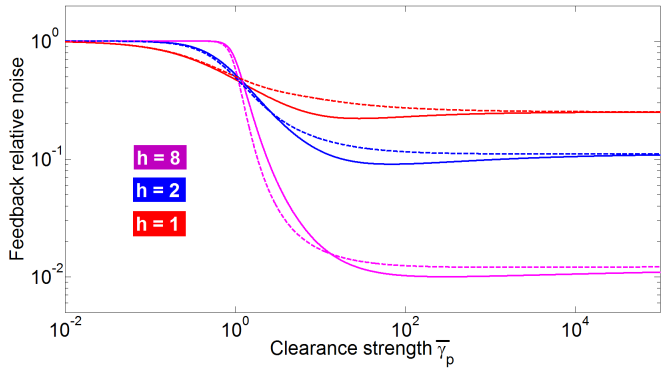

Fig. 6. Feedback relative noise versus the clearance strength $\overline{\gamma}_p$ for different values of the feedback sensitivity. The Hill coefficient has been fixed to $h = 4$. Fixed parameters (k_p, k_e, γ_p, γ_e, θ) are reported in Table II. Continuous lines refer to $n = 2$; dotted lines refer to $n = 12$.

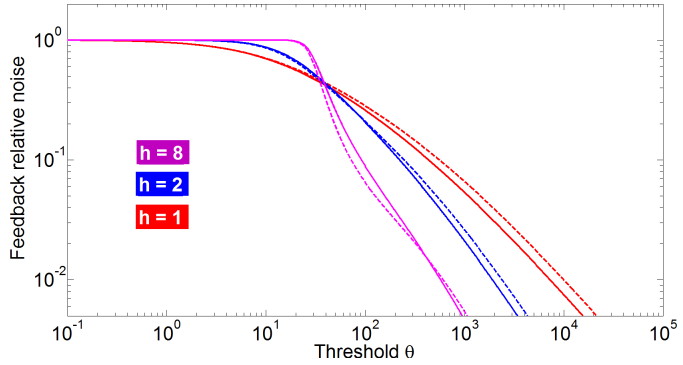

Fig. 7. Feedback relative noise versus the threshold θ for different values of the feedback sensitivity. The Hill coefficient has been fixed to $h = 4$. Fixed parameters (k_p, k_e, γ_p, γ_e, θ) are reported in Table II. Continuous lines refer to $n = 2$; dotted lines refer to $n = 12$.

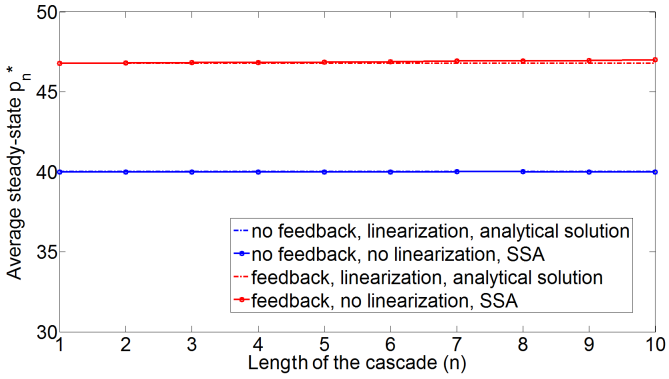

Fig. 8. Average steady-state ϱ versus the length of the cascade n. Comparison between linearized SHS results and non-linearized Gillespie numerical simulation. All parameters (except n) are fixed to the values of Table II.

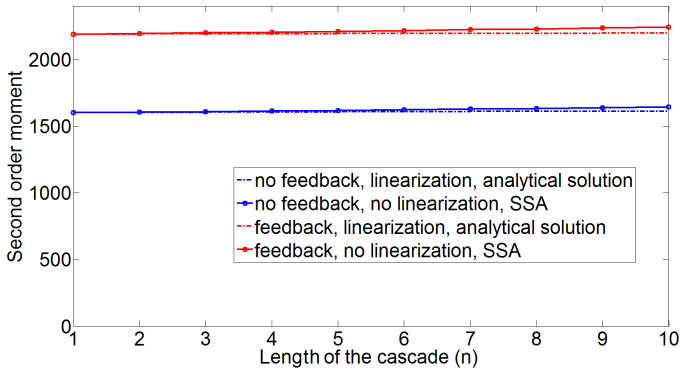

Fig. 9. Second order moments $\langle p_n^2 \rangle^\star$ versus the length of the cascade n. Comparison between linearized SHS results and non-linearized Gillespie numerical simulation. All parameters (except n) are fixed to the values of Table II.

simulations are carried out without the linearization and are very close to the linear SHS approximation: they apparently show that the linear approximation adopted to achieve closed moment equations with SHS is a reasonable tradeoff to lighten the computational burden, still keeping meaningful results.

VI. Conclusions

In this note, a study on noise propagation in a class of metabolic networks has been carried out. The biological system under investigation is a cascade of metabolic reactions, eventually leading to the formation of a final product by means of intermediate substrate transformations. The formalization adopted is a Stochastic Hybrid System (linearized in order to achieve closed moment equations), with the only noise source provided by the production/clearance processes associated to the copy number variations of the enzyme e. Noise propagation has been investigated with respect to the length of the cascade and with respect to the action exerted in feedback on the final product clearance rate by the product accumulation itself. In addition to showing the unmistakable role of the feedback in noise reduction (a positive feedback, in this case), analytical results allow to investigate the impact of different model parameters on noise regulation where, in particular, an interesting result correlates the impact of the length n of the cascade to the enzyme dynamics.

Acknowledgements

PP is supported by the MIUR grant SysBioNet Italian Roadmap for ESFRI Research Infrastructures, SYSBIO Centre of Systems Biology, Milan and Rome, Italy.

AS is supported by the National Science Foundation Grant DMS-1312926.

References

[1] D.H. Calhoun, G.W. Hatfield, Autoregulation: a role for a biosynthetic enzyme in the control of gene expression, *Proceedings of the National Academy of Sciences* 70.10 (1973): 2757-2761.

[2] G. Stephanopoulos, A. Aristidou, J. Nielsen, *Metabolic Engineering: Principles and Methodologies*, Academic Press, San Diego, CA, 1998.

[3] A. Zaslaver, A. Mayo, R. Rosenberg, P. Bashkin, H. Sberro, M. Tsalyuk, M. Surette, U. Alon, Just-in-time transcription program in metabolic pathways, *Nat. Genet.* 36, 486-491, 2004.

[4] U. Alon, *An Introduction to Systems Biology: Design Principles of Biological Circuits*, Chapman and Hall/CRC, 2006.

[5] A. Singh, J.P. Hespanha, Optimal feedback strength for noise suppression in autoregulatory gene networks, *Biophysical Journal* 96, 4013-4023, 2009.

[6] W.J. Holtz, J.D. Keasling, Engineering static and dynamic control of synthetic pathways, *Cell*, 140, 19–23, 2010.

[7] Oyarzun, D.A, Lugagne, J.-B., Stan, G.-B.V.: Noise propagation in synthetic gene circuits for metabolic control, ACS Synthetic Biology, 2014.

[8] A. Borri, P. Palumbo, A. Singh, Impact of negative feedback in metabolic noise propagation, *IET Syst. Biol.*, 1-8, 2016.

[9] A. Borri, P. Palumbo, A. Singh, Metabolic noise reduction for enzymatic reactions: the role of a negative feedback, *Proceedings of the 54th IEEE Conference on Decision and Control (CDC 2015)*, Osaka, Japan, pp. 2537–2542, 2015.

[10] A. Borri, P. Palumbo, A. Singh, Noise reduction for enzymatic reactions: a case study for stochastic product clearance, *Proceedings of the 55th IEEE Conference on Decision and Control (CDC 2016)*, Las Vegas, USA, pp. 5851–5856, 2016.

[11] E.D. Sontag, Some new directions in control theory inspired by systems biology, *Syst. Biol.* 1(1) (2004): 9-18.

[12] D.E. Cameron et al, A brief history of synthetic biology, *Nat. Rev. Microbiol.*, 12, 381–390, 2014.

[13] D. Del Vecchio, and E. D. Sontag, Synthetic biology: A systems engineering perspective, *Control Theory and Systems Biology*, 101–124, 2009.

[14] D. Del Vecchio, A. J. Ninfa, and E. D. Sontag, Modular cell biology: retroactivity and insulation, *Molecular systems biology*, 4.1, 161, 2008.

[15] D. Del Vecchio, Modularity, context-dependence, and insulation in engineering biological circuits, *Trends in Biotechnology*, 33(2), 111–119, 2015.

[16] D. Del Vecchio, A.J. Dy, Y. Qian, Control theory meets synthetic biology, *J. R. Soc. Interface* 13, 13: 20160380. http://dx.doi.org/10.1098/rsif.2016.0380

[17] D.J. Kiviet, P. Nghe, N. Walker, S. Boulineau, V. Sunderlikova, S.J. Tans, Stochasticity of metabolism and growth at the single-cell level. *Nature*, 514, 376–379, 2014.

[18] A. Singh and J. P. Hespanha, Scaling of stochasticity in gene cascades, Proceeding of the American Control Conference (ACC 2008), Seattle, WA, pp. 2780-2785, 2008.

[19] J.P. Hespanha, A. Singh, Stochastic models for chemically reacting systems using polynomial stochastic hybrid systems, *Int. J. of Robust and Nonlinear Control*, 15, 669-689, 2005.

[20] A. Singh, J.P. Hespanha, Approximate moment dynamics for chemically reacting systems, *IEEE Transactions on Automatic Control.* 56, 414-418, 2011.

[21] E. D. Sontag and A. Singh, Exact Moment Dynamics for Feedforward Nonlinear Chemical Reaction Networks, in IEEE Life Sciences Letters, vol. 1, no. 2, pp. 26-29, Aug. 2015.

[22] D. T. Gillespie, Exact Stochastic Simulation of Coupled Chemical Reactions, *The Journal of Physical Chemistry* 81(25), 23402361, 1977.